ACCOUNTS
of chemical research

Dextran-Coated Iron Oxide Nanoparticles: A Versatile Platform for Targeted Molecular Imaging, Molecular Diagnostics, and Therapy

CARLOS TASSA, STANLEY Y. SHAW, AND RALPH WEISSLEDER*

Center for Systems Biology, Massachusetts General Hospital and Harvard Medical School, Boston, Massachusetts 02114, United States

RECEIVED ON MARCH 15, 2011

CONSPECTUS

Advances in our understanding of the genetic basis of disease susceptibility coupled with prominent successes for molecular targeted therapies have resulted in an emerging strategy of personalized medicine. This approach envisions risk stratification and therapeutic selection based on an individual's genetic makeup and physiologic state (the latter assessed through cellular or molecular phenotypes). Molecularly targeted nanoparticles can play a key role in this vision through noninvasive assessments of molecular processes and specific cell populations in vivo, sensitive molecular diagnostics, and targeted delivery of therapeutics.

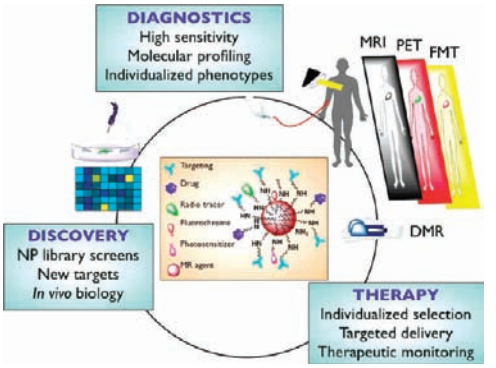

A superparamagnetic iron oxide nanoparticle with a cross-linked dextran coating, or CLIO, is a powerful and illustrative nanoparticle platform for these applications. These structures and their derivatives support diagnostic imaging by magnetic resonance (MRI), optical, and positron emission tomography (PET) modalities and constitute a versatile platform for conjugation to targeting ligands. A variety of conjugation methods exist to couple the dextran surface to different functional groups; in addition, a robust bioorthogonal [4 + 2] cycloaddition reaction between 1,2,4,5-tetrazene (Tz) and *trans*-cyclooctene (TCO) can conjugate nanoparticles to targeting ligands or label pretargeted cells. The ready availability of conjugation methods has given rise to the synthesis of libraries of small molecule modified nanoparticles, which can then be screened for nanoparticles with specificity for a specific cell type. Since most nanoparticles display their targeting ligands in a multivalent manner, a detailed understanding of the kinetics and affinity of a nanoparticle's interaction with its target (as determined by surface plasmon resonance) can yield functionally important insights into nanoparticle design.

In this Account, we review applications of the CLIO platform in several areas relevant to the mission of personalized medicine. We demonstrate rapid and highly sensitive molecular profiling of cancer markers ex vivo, as part of detailed, individualized molecular phenotyping. The CLIO platform also facilitates targeted magnetic resonance and combined modality imaging (such as MR/PET/fluorescence/CT) to enable multiplexed measurement of molecular phenotypes in vivo for early diagnosis and disease classification. Finally, the targeted delivery of a photodynamic therapy agent as part of a theranostic nanoparticle successfully increased local cell toxicity and minimized systemic side effects.

1. Introduction

Advances in our understanding of the genetic basis of disease susceptibility, coupled with prominent successes for molecular targeted therapies, have resulted in an emerging strategy of personalized medicine. This approach envisions risk stratification and therapeutic selection based on an individual's genetic makeup and physiologic state (the latter assessed through cellular or molecular phenotypes). Molecularly targeted nanoparticles can play a key role in this vision through noninvasive assessments of molecular processes and specific cell populations in vivo, sensitive molecular diagnostics ex vivo, and targeted delivery of therapeutics.[1−3] Derivatized dextran coated magnetic nanoparticles[4,5] are a powerful platform for these applications, as they support diagnostic imaging by magnetic resonance (MRI), optical, and positron emission tomography (PET)

Published on the Web 06/10/2011 www.pubs.acs.org/accounts
10.1021/ar200084x

modalities, and constitute a versatile platform for conjugation to targeting ligands. Pharmacokinetic and toxicity studies have revealed these nanomaterials to be sufficiently nontoxic and biodegradable[6,7] with extended vascular retention times. Certain nanoparticles of this class are now FDA-approved.

Experimental dextran-coated superparamagnetic iron oxide nanoparticles are a well-established platform for the synthesis of multifunctional imaging agents. These include monocrystalline iron oxide nanoparticles (or MION)[8,9] and the related nanoparticles where the dextran is covalently cross-linked (cross-linked iron oxide nanoparticles, or CLIO) to form amine groups that are ready substrates for conjugation to targeting ligands. Several nanoparticles with iron cores and carbohydrate coatings have been approved for human use. In 1996, the United States Food and Drug Administration (FDA) approved Feridex I.V. (ferumoxides) as the first nanoparticle-based iron oxide imaging agent for the detection of liver lesions. A smaller monodisperse version Combidex (ferumoxtran-10) has been used to image occult prostate cancer lymph-node metastases in humans. Finally, Feraheme (ferumoxytol) has been approved to treat iron deficiency anemia in adult patients with chronic kidney disease. Ferumoxytol is also under clinical investigation for the detection of central nervous system (CNS) inflammation, brain neoplasms, and cerebral metastases from lung or breast cancer.

This Account will describe our recent efforts in the development of an integrated system of nanoparticles, conjugation chemistries, screening methods, and detection technologies, with wide applications in biologic discovery, molecular imaging, diagnostic analyte detection, and therapeutic decision-making and monitoring.

2. CLIO Platform

Superparamagnetic iron oxide nanoparticles are typically produced by one of two different mechanisms: (i) high temperature hydrophobic crystal growth and subsequent coating with biocompatible polymers[10−13] or (ii) precipitation from an alkaline solution containing a mixture of iron salts (Fe^{2+}, Fe^{3+}) and a coating polymer such as dextran.[4] The former generally results in highly monodisperse, high relaxivity materials primarily used for in vitro applications,[14] and the latter results in much more biocompatible materials for in vivo use.[6,15,16]

MION are produced by the second method and contain a 3−5 nm monocrystalline core surrounded by a layer of dextran of variable thickness. The overall mean hydrated diameter typically falls within the 20−45 nm range. Since the iron core and dextran shell are held together via noncovalent binding interactions, core−shell dissociation may occur under certain biological conditions. To prevent dextran dissociation and introduce a convenient functional group for multivalent conjugation, MION can be treated with epichlorohydrin to cross-link the dextran coating (resulting in cross-linked iron oxide nanoparticles, or CLIO) followed by treatment with ammonia to introduce primary amines (CLIO-NH_2).[8,9] The primary amines distributed throughout the nanostructure allow increased loading capacity for the attachment of multiple targeting ligands, imaging agents, and therapeutics into one entity. An alternative to chemical cross-linking is the use of carboxylated dextrans as the primary coating.[17,18]

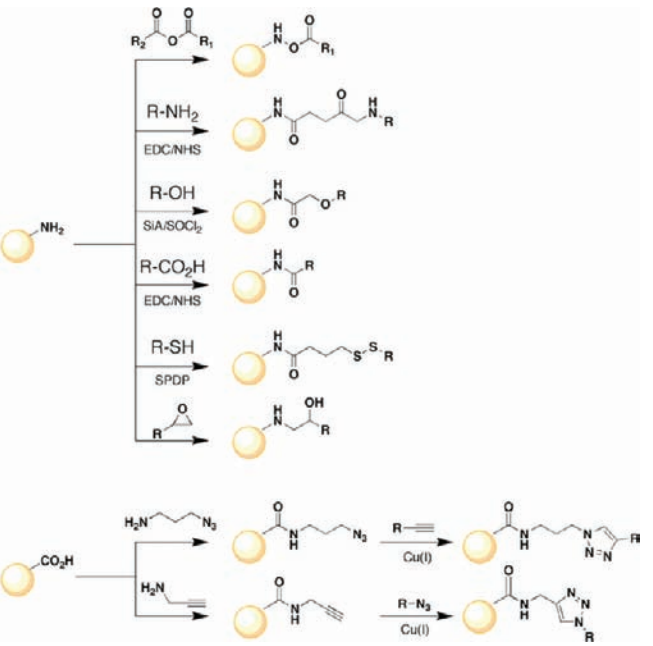

FIGURE 1. Conjugation chemistries to attach small molecules to CLIO. Figure reproduced with permission from Shaw, S.Y. Chemical Biology Approaches to Molecular Imaging. In Molecular Imaging: Principles and Practice (Weissleder, R., Ross, B. D., Rehemtulla, A., Gambhir, S. S.; Eds.), People's Medical Publishing House: Shelton, CT, USA, 2010; pp 497−508.

3. Chemistry

Efficient conjugation chemistry methods have extended the versatility of the CLIO platform for multiple applications. Straightforward protocols exist to conjugate ligands bearing a variety of functional groups to the primary amines on CLIO's dextran coating, including anhydrides, amines, hydroxyls, carboxylic acids, thiols, and epoxides (Figure 1). Recently, a bioorthogonal [4 + 2] cycloaddition reaction

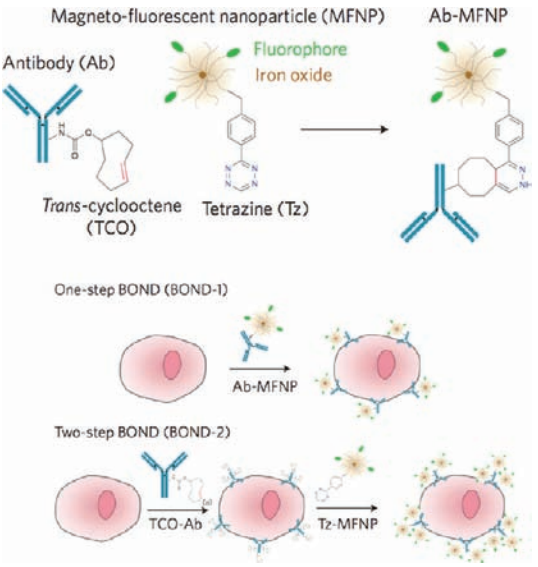

FIGURE 2. Bioorthogonal [4 + 2] cycloaddition reaction between 1,2,4,5-tetrazene (Tz) and *trans*-cyclooctene (TCO) for labeling of nanoparticles (top) or cell surfaces (bottom). Figure was reproduced with permission from ref 22. Copyright 2010 Nature Publishing Group.

between 1,2,4,5-tetrazene (Tz) and *trans*-cyclooctene (TCO) was described that can label cancer cells, peptides, and small molecules.[19−21] (Figure 2). The reaction does not require catalyst, and it proceeds rapidly at room temperature with high yields in a variety of solvents including serum. A novel labeling strategy termed BOND for "bioorthogonal nanoparticle detection" uses this mechanism to conjugate nanoparticles to targeting ligands such as antibodies (Figure 2).[22,23] Antibodies are modified with TCO moieties at lysine residues. TCO-modified antibodies can then be reacted with Tz-derivatized nanoparticles, resulting in multivalent nanoparticles bearing multiple copies of targeting ligands (e.g., antibodies, peptides, or small molecules). To maximize the amplification conferred by multivalent attachment, it may be advantageous to use reactants and ligands that impose minimal steric hindrance (small "footprints") and allow a maximal number of covalent attachment sites on the nanoparticle. BOND type chemistry enables efficient targeting and signal amplification for a wide variety of diagnostic and detection applications.[24−28]

4. Small-Molecule Modified Nanoparticle Libraries

While most CLIO-based applications to date have utilized peptides or antibodies for targeting, surface modification through multivalent attachment of small molecules holds great potential for selective targeting of cell types. The flexible CLIO platform enables a screening approach to be extended to libraries of small-molecule-modified nanoparticles, that is, phenotypic screens to identify targeted nanoparticles with specificity for a cell-type of interest (and without a priori knowledge of the protein target). Phenotype-driven screens of nanoparticle libraries are a powerful complement to traditional target-based nanoparticle design and may enable targeting of a broader range of cell types of interest.

As an example, amino CLIO (bearing ~62 free amines) was sparsely labeled with the near IR fluorochrome Cy5.5. Remaining free amines were conjugated to 146 different small molecules (MW < 500 Da) selected based on water solubility and chemical diversity.[29] While the starting CLIO nanoparticle is taken up exclusively by macrophages, screening in different cell lines and subsequent studies showed that glycine-modified CLIO specifically labeled functional macrophage subsets, such as a subset of tumor-associated macrophages with proangiogenic and immunosuppressive properties.[30]

While the above study narrowed nanoparticle targeting from all macrophages to a functional macrophage subset, a long-term goal is to enable targeting of nonmacrophage cell types. A subsequent study demonstrated the viability of this approach, by screening for small molecule-modified nanoparticles with enhanced binding to vascular endothelial cells. The robustness of the screen was increased by several design elements (a) using primary isolates of human endothelial cells (rather than cell lines), (b) screening multiple independent isolates of endothelial cells from multiple vascular beds (to avoid skewing screening results by a single idiosyncratic cell isolate, and enhance the generality of screening "hits"), and (c) by adopting rigorous analytic methods for the multidimensional data set.[31] Nanoparticles were screened for enhanced binding to 11 isolates of vascular endothelial cells (the target class), while minimizing binding to 2 isolates of macrophages (background class). A *t*-statistic was calculated for each nanoparticle, which reflects the extent that the nanoparticle shows a difference in binding to endothelial cells, compared to its binding to macrophages. The statistical significance for each nanoparticle was evaluated using permutation-based *p*-values (Figure 3). From the "hits" from the initial screen ($p \leq 3 \times 10^{-3}$), selected nanoparticles were validated by demonstrating enhanced localization to endothelium in two physiologic contexts: human carotid endarterectomy samples (from operating room specimens) and intravital imaging of murine blood vessels in vivo. Thus, phenotypic cell-based screening of nanoparticle libraries across target versus background cell types, combined with appropriate analytic methods, led to the discovery of imaging probes with novel properties.

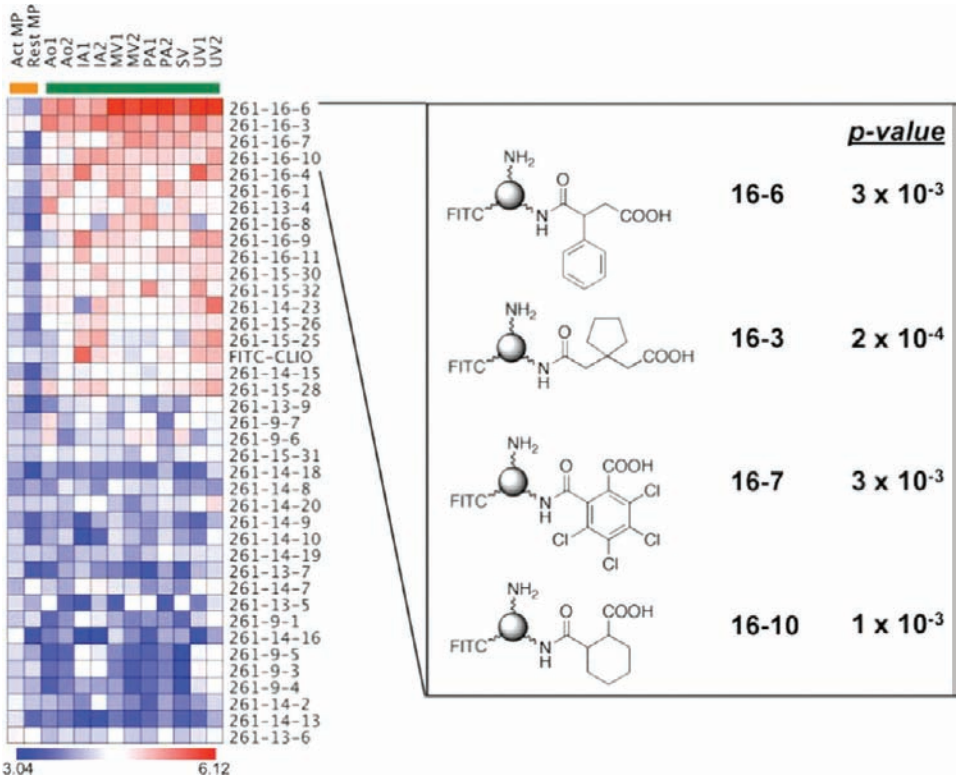

FIGURE 3. Screening for small-molecule-modified nanoparticles with enhanced binding to 11 independent endothelial isolates (relative to macrophage binding). Figure reproduced with permission from ref 31. Copyright 2009 RSC Publishing.

These unbiased screening approaches can be extended to identify probes for a wide variety of cell types of interest. In the context of personalized medicine, one could envision screens for imaging probes that distinguish cells defined by a difference in phenotype (e.g., low vs high metastatic potential) or genotype (e.g., expressing a risk allele vs a protective allele at a disease gene).

5. Ligand Effects on Nanoparticle Binding

Targeted nanoparticles are widely thought to benefit from multivalent interactions, where multiple ligands on the nanoparticle simultaneously bind to multiple receptors on another entity (e.g., a cell surface or a multimeric protein).[32] However, given the complexities inherent in the interactions of nanoparticle surfaces with their targets, and the structural diversity of nanoparticle scaffolds and targeting ligands, our understanding of how the multivalent display of targeting ligands affects nanoparticle binding remains incomplete. Furthermore, the effects of multivalency on nanoparticle binding are often not quantitated or are measured indirectly through cell-based assays.

To address these issues, we used surface plasmon resonance (SPR) to directly quantitate the affinity and kinetics of nanoparticle−target interactions in real time.[33] We studied a deliberately constrained system where CLIO was conjugated to a series of structurally related synthetic analogues that all bound the same target, FK506-binding protein 12 (FKBP12). The K_D's for the free FKBP12 ligands span a 4500-fold range (24 nM to 110 μM). These FKBP12 ligands were conjugated to CLIO using sulfhydryl exchange chemistry, which allowed quantitative determination of ligand loading and thus nanoparticle multivalency (ranging from ~3−18 ligands/CLIO). At high receptor (FKBP12) densities typically used for SPR experiments, multivalent interactions resulted in negligible dissociation rates (k_d). However, at lower, physiologically relevant receptor densities (comparable to measured receptor densities on cancer cells), several notable findings resulted (Figure 4). As expected, dissociation rates k_d between the multivalent nanoparticle and FKBP12 were significantly reduced relative to the free small molecule ligands. Less expected was the considerable variation in association rates, as k_a for the nanoparticle−FKBP12 interaction increased, decreased, or remained largely unchanged relative to the free small molecules. Quantitative curve-fitting of SPR responses confirmed that increasing contributions from multivalent (as opposed to monovalent) interactions correlated

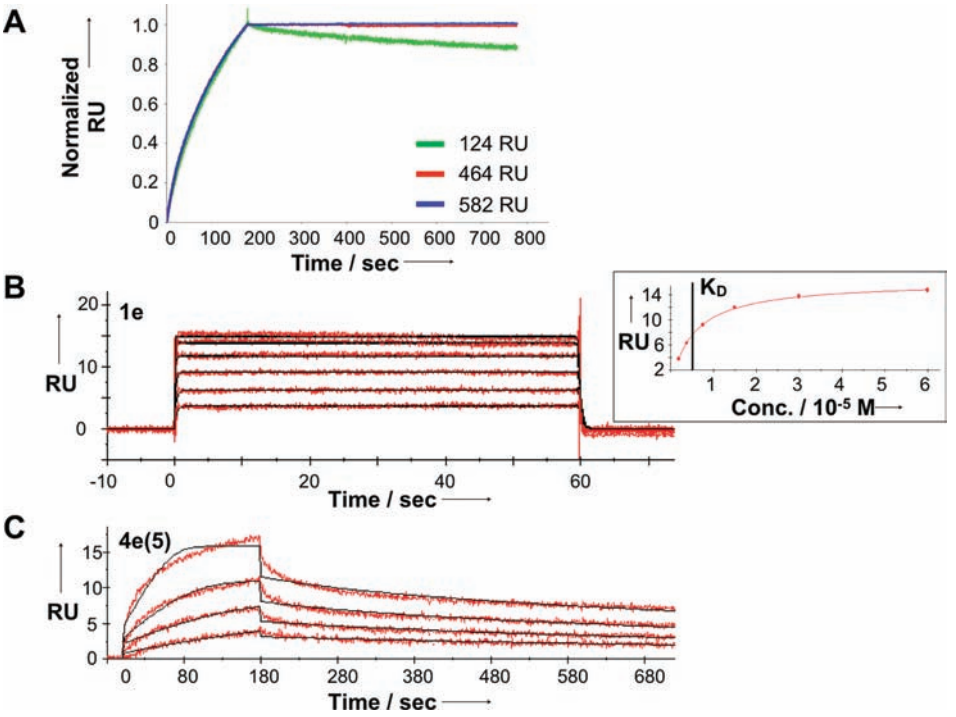

FIGURE 4. Surface plasmon resonance to quantitate kinetics and affinity of nanoparticle binding. (A) At high target densities (e.g., 464 and 582 RU, or response units), there is negligible dissociation of multivalent nanoparticles. (B, C) SPR reveals distinct kinetics for interaction of a protein target with its free small molecule ligand (B) vs a multivalent nanoparticle conjugated to the ligand (C). Figure reproduced with permission from ref 33. Copyright 2010 American Chemical Society.

with increased binding affinity and avidity. Parallel analyses showed that structural components such as linker length and conjugation chemistry could also influence binding kinetics of multivalent nanoparticles in unexpected ways.

The kinetic insights uncovered by our SPR measurements at physiologically relevant receptor densities could have important functional implications. First, they suggest that nanoparticle design may not always be straightforwardly modular, as the details of how a nanoparticle is conjugated to a targeting ligand influenced nanoparticle behavior. Second, they argue that direct measurement of nanoparticle binding affinities and kinetics can inform nanoparticle design. For instance, nanoparticle affinity, and association and dissociation rates can all affect how deeply an intravascular circulating agent penetrates into tissue before its target sites become effectively saturated;[34] the relative contribution of these variables depends on several in vivo factors, including capillary permeability, particle size, and target density. In light of this, two targeted nanoparticles that have comparable equilibrium affinities for their target may possess very distinct kinetic properties with functional consequences. More broadly, SPR can guide the design, synthesis, and structure–activity studies of functionalized nanoparticles for a variety of ligand, scaffold, and target combinations.

6. Biomedical Applications

Progress in the syntheses of nanoscale materials is envisioned to play a critical role in the development of novel diagnostics and therapeutics. Derivatized magnetic nanoparticles (with carbohydrate coatings such as dextran) possess many properties that make them well-suited for these applications. The superparamagnetic iron oxide core enables in vivo imaging by magnetic resonance. Clustering of nanoparticles can be used as the basis for highly sensitive ex vivo analyte detection in point-of-care devices. The nanoparticle surfaces are readily modified with targeting ligands and can benefit from enhanced avidity conferred by multivalency. Antibody, peptide, and/or small molecule derivatized magnetic nanoparticles have all been developed successfully. The particles are biocompatible, with favorable circulating half-lives. For all of these reasons, these nanoparticles are widely utilized in translational cell- and animal-based experiments, and certain nanoparticles of this class are now FDA approved for human use. The sections below briefly summarize some recent highlights; further details may be found in several reviews.[2,35,36]

6.1. Diagnostic Magnetic Resonance (DMR). The ability to detect specific analytes in a sensitive and efficient manner is critical for point of care tests for diagnosis, prognosis, and

monitoring of disease activity and therapeutic efficacy. Ideal biosensors should provide rapid, high sensitivity detection and quantitation of a range of different analytes, with low sample volume requirements and cost. An innovative approach for detecting analytes takes advantage of CLIO-like nanoparticles and magnetic self-amplifying proximity effects[37] or magnetic tagging.[14,38,39] In either mode, the presence of the target analyte induces target-mediated nanoparticle clustering, resulting in decreased T_2 relaxation times or increased relaxation rates R_2 ($R_2 = 1/T_2$) of neighboring water molecules relative to monodisperse nanoparticles (forward magnetic relaxation switching, or MRS). Several different types of molecular interactions have been detected using MRS and benchtop relaxometers, including DNA−DNA, protein−protein, protein−small molecule, enzymatic activity via reverse assay, telomerase activity, and bacterial detection.[37,40−45] Significantly, these can be detected in turbid media and whole cell lysates; the lack of purification is a critical advantage for processing of clinical samples such as blood. In a recent study addressing the effects of multivalency on the binding and detection of cells using magnetic relaxation nanosensors, high valency nanoparticles outperformed the low valency counterpart, achieving rapid single cell detection.[46] Additionally, multivalent nanosensors have been used as molecular mimics for toxin detection.[47]

Miniaturization of the magnetic resonance components has resulted in a field-ready diagnostic magnetic resonance (DMR) device.[38] The first prototype, DMR-1, incorporates a microcoil array, microfluidic network, electronics, and permanent magnet, all in a portable self-contained assembly. Onboard custom electronics provide both longitudinal (T_1) and traverse (T_2) relaxation time measurements. Side-by-side performance comparisons between a benchtop relaxometer and DMR-1 showed less than 2% difference in measured *R*1 and *R*2 values. (relaxation per iron concentration in water). Moreover, DMR-1 mass detection sensitivity improved 80-fold over the relaxometer, due mainly to device miniaturization which enables stronger radio frequency field generation with increased filling factors in small sample volumes.

A second generation device, DMR-2, improved detection sensitivity.[14] First, the probe design was changed to a solenoid microcoil probe embedded in a microfluidic structure to decrease sample volume and improve signal-to-noise ratio (SNR). The second improvement took advantage of novel water-soluble magnetic nanoparticles (MNP) with significantly greater r_2 relaxivities (high r_2 will induce large R_2 changes) which were synthesized by doping iron oxide

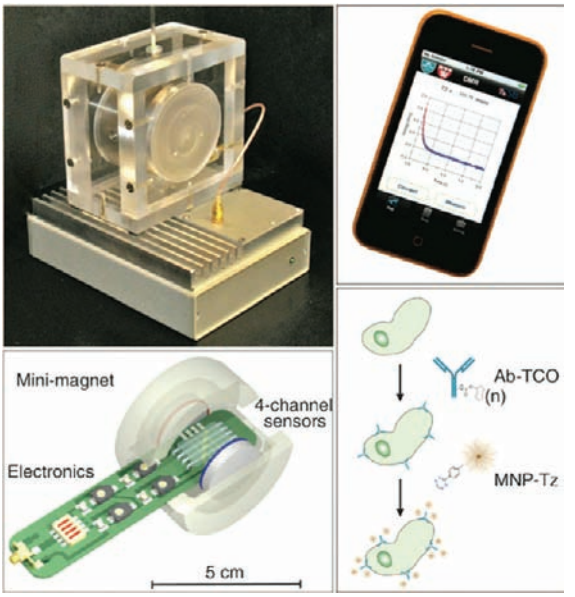

FIGURE 5. μNMR diagnostic magnetic resonance (DMR) device. Point-of-care μNMR device (top left) containing circuitry for NMR measurements (bottom left) is controlled by a smartphone application. Detection of cellular receptors via magnetic nanoparticles and BOND bioorthogonal conjugation is shown at bottom right. Figure reproduced with permission from ref 48. Copyright 2011 American Association for the Advancement of Science.

nanoparticles with manganese (Mn-MNP) and using seed-growth techniques to increase overall metallic core size. In fine needle aspirates (FNAs) from xenograft mouse tumors, DMR-2 combined with anti-Her2/neu-Mn-MNP nanoparticles resulted in a linear relationship between traverse relaxation rate R_2 and Her2/neu$^+$ cell counts, with a detection limit of ~2 cells per 1 uL sample (far below that of standard-of-care methods such as histology).

Finally, a third generation device (DMR-3) is an integrated, clinical micro-NMR (μNMR) device capable of rapid and quantitative profiling of multiple protein markers[48] (Figure 5). DMR-3 includes the capability to perform multiplexed analyte measurement, microfluidic specimen delivery, and increased temperature stability, and can be controlled via a smartphone application. Cells from FNAs for suspected human abdominal malignancies were first labeled by a TCO-modified antibody against the cancer marker, followed by labeling with Tz-modified magnetic nanoparticles. This system was first used to profile 9 different cancer markers in 50 patients undergoing abdominal FNA (Figure 6). μNMR signals for the cancer markers showed very high correlation with gold-standard methods of clinical measurement, such as flow cytometry or immunohistochemistry. Using standard-of-care clinical assessments classifying each tumor as benign or malignant as the

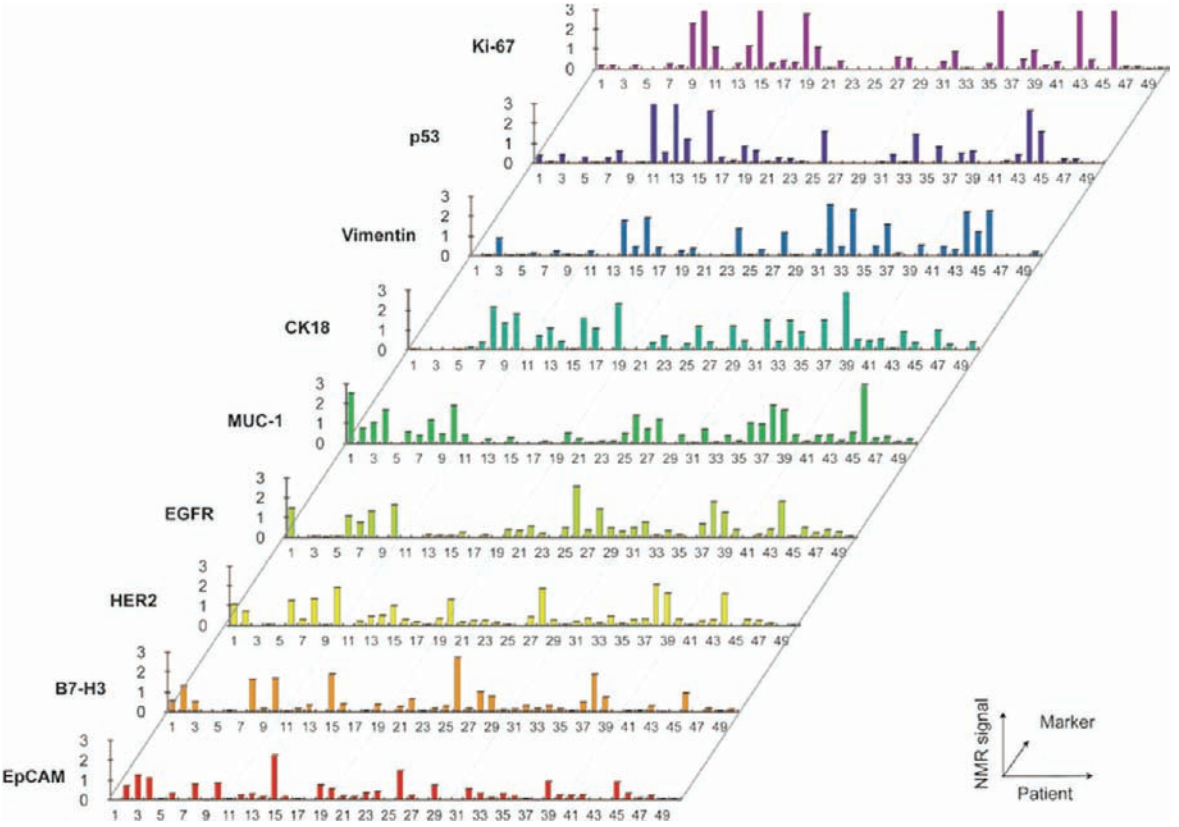

FIGURE 6. Profiling of cancer marker expression from 50 patient FNAs using DMR. Figure reproduced with permission from ref 48. Copyright 2011 American Association for the Advancement of Science.

gold standard, a weighted four-marker profile (composed of MUC-1, EGFR, HER2, and EpCAM) showed 96% accuracy. In an independent cohort of 20 patients, this four-marker panel showed 100% accuracy in classifying samples as benign or malignant. Of note, marker measurements by μNMR were available in less than 1 h, while standard processing required 3−4 days on average and often longer. Thus, sensitive detection of cells from human FNAs using DMR-3 and magnetic nanoparticles can enable patient phenotyping based on profiles of expressed cancer markers. DMR-3 enables a binary diagnostic distinction (benign vs malignant), but the underlying approach is adaptable to multiplex phenotyping of patient tumors for tumor classification, risk stratification, and monitoring response to therapy.

6.2. Magnetic Resonance Imaging (MRI). The ability to image CLIO and related nanoparticles by magnetic resonance has led to several probes that image cellular and subcellular events with high spatial resolution,[6,17,49−65] and can be used for early diagnosis, risk stratification, and monitoring of disease activity or therapeutic efficacy. For example, a magnetofluorescent nanoparticle targeted to vascular adhesion molecule-1 (VCAM-1) was designed to image atherosclerosis in vivo.[60] Upregulation of vascular adhesion molecule-1 (VCAM-1) on activated endothelial cells, macrophages, and smooth muscle cells is an early marker of atherosclerosis. A VCAM-1 targeting peptide was selected utilizing iterative phage display, and conjugated to CLIO. Intravenous administration of this targeted particle results in enhanced MR signal in aortic roots of apoE$^{-/-}$ mice, which correlated with VCAM-1 expression. This probe was also useful for in vivo monitoring of therapeutic efficacy, as evidenced by improved signal after statin treatment.

In another example, a similar magnetofluorescent nanoparticle was designed to visualize apoptosis. Phosphatidylserine becomes externalized on cell membranes early in the apoptotic process, and annexin V binds phosphatidylserine. CLIO conjugated to annexin V has been shown to be a sensitive indicator of cardiomyocyte apoptosis in vivo.[62−64]

6.3. Positron Emission Tomography (PET) Imaging. Positron emission tomography (PET) imaging identifies high-energy photons from trace quantities of decaying radioactive isotopes with significantly higher sensitivity than MRI. Labeling of nanoparticles with PET isotopes such as ^{18}F has been

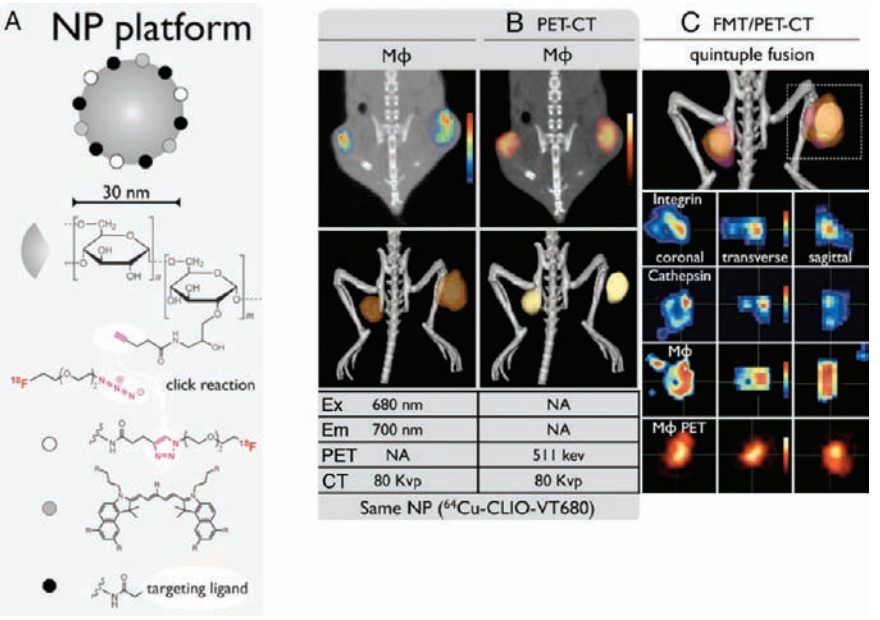

FIGURE 7. Multimodal PET imaging using nanoparticles. (A) Versatile conjugation capabilities of CLIO, e.g., to ^{18}F using click chemistry, but also to peptides or other targeting ligands. (B, C) In vivo multichannel PET-CT (B) and FMT/PET-CT (C) of tumor-bearing mice, coinjected with fluorescent peptide against integrins, a fluorescent cathepsin sensor, and ^{64}Cu-CLIO-VT680 (labeling macrophages). Figure reproduced with permission from ref 66. Copyright 2010 National Academy of Sciences.

successfully used to decrease both the detection threshold and the clinical dose required. Using copper-catalyzed azide−alkyne cycloaddition ("click" chemistry), a fluorescently derivatized CLIO was conjugated with ^{18}F to create a trimodal nanoparticle that can be detected by PET, fluorescence molecular tomography (FMT) and MRI (Figure 7). The detection threshold for ^{18}F-CLIO by PET was 200 times more sensitive than that of MRI[16] and 50 times more sensitive than that of FMT. In agar-based phantoms, CLIO-based particles bearing ^{18}F and the fluorescent dye VT680 show excellent correlation between PET and FMT signals ($r^2 > 0.99$).

CLIO-based PET/FMT/MRI imaging agents offer the prospect of sensitive, multichannel assessments of different biological signals in vivo. In a CT26 colon carcinoma mouse xenograft model, ^{64}Cu-CLIO-VT680 showed good correlation of PET and FMT signals ($r^2 = 0.82$) within tumor volumes, corresponding to CLIO targeting of tumor-associated macrophages. For multichannel imaging in vivo, the ^{64}Cu-CLIO-VT680 particle was coinjected with a fluorescent probe for cathepsin enzymatic activity and a fluorescent probe for $\alpha v\beta 3$ integrins. Spectrally resolved signals were observed within tumors in vivo, with different agents localizing to distinct subregions of the tumor according to their biological targets[66] (Figure 7).

PET-CT imaging of ^{18}F-CLIO resulted in significantly higher PET signal in murine aortic aneurysms compared to normal aorta, due to ^{18}F-CLIO targeting of monocytes and macrophages within the aneurysm. Cellular probe distribution was validated by radionuclide, fluorescence, histologic, and flow cytometric measurements. Currently, decisions on surgical resection of aneurysms are based on population-derived risk factors such as aneurysm diameter. Nanoparticle−PET agent conjugates may allow individualized therapeutic decisions, based on molecular disease markers such as cellular inflammatory activity in the aneurysm.[67]

6.4. Theranostic Particles: Photodynamic Therapy (PDT). Various formulations of iron-oxide-based nanoparticles have been developed for theranostic applications, in which the nanoparticle carries imaging, targeting, and therapeutic capabilities. For instance, iron oxide nanoparticles were synthesized with a poly(acrylic acid) (PAA) polymer coating that encapsulated a near-infrared dye and the chemotherapeutic drug Taxol. Functionalization of this nanoparticle with folate allowed uptake into A549 lung cancer cells, Taxol release, and cell death.[68] Nanoparticle-borne payloads have included genes, proteins, drugs, or combinations thereof, which have recently been reviewed.[69]

PDT is a promising treatment modality for several types of diseases including artherosclerosis and cancer.[70] PDT uses a photosensitizer-based drug, oxygen, and light of a specific wavelength to produce singlet oxygen, a highly reactive species that causes proximity-based photonecrotic effects. By directing light of a specific wavelength to a precise

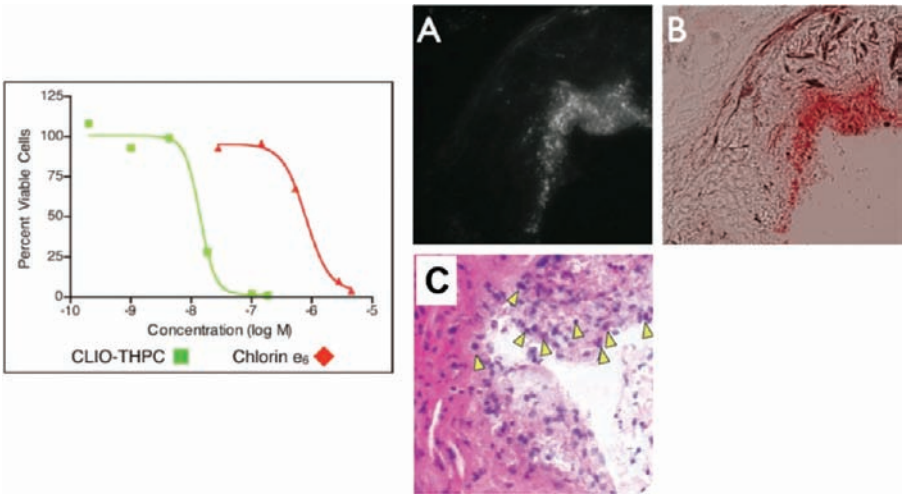

FIGURE 8. Nanoparticle-based theranostic agent for photodynamic therapy. (Left) Theranostic nanoparticle enhances phototoxicity vs chlorin e_6. (Right) CLIO-THPC localizes to atheroma of apoE$^{-/-}$ mice, as evidenced by fluorescent microscopy of nanoparticle (A), merged fluorescent-bright field microscopy (B), and areas of apoptotic and necrotic cells (C). Figure reproduced with permission from ref 73. Copyright 2010 Wiley-VCH.

region, PDT can cause localized tumor killing without damaging nearby healthy tissue. A drawback to systemically delivered photosensitizers, however, is skin accumulation leading to photosensitivity.

CLIO has proven to be an appealing theranostic platform to deliver photosensitizing agents in a targeted fashion, decreasing photosensitivity complications. Hydroporphyrins of the chlorin class sensitize formation of singlet oxygen and have been used extensively in PDT applications.[71] In a first generation multimodal theranostic nanoparticle (TNP), CLIO was conjugated to the potent photosensitizer tetraphenyl-2,3-dihydroxychlorin (TPC) (with singlet oxygen quantum yield = 0.65 (645 nm excitation)), and also to Alexa Fluor 750 for fluorescent localization.[72] The resulting TNP had a characteristic UV−vis absorption spectrum featuring all three optically active components (CLIO abs < 400 nm, TPC abs = 650, and Alexa Fluor 750 abs = 750). The 100 nm differences in absorption between TPC and Alexa Fluor 750 minimized energy transfer and singlet oxygen generation during optical imaging. In a macrophage cell line, irradiation with 650 nm light resulted in dose-dependent phototoxicity, whereas irradiation at 750 nm for optical imaging did not cause any observable cell death.

A second-generation TNP conjugated the hydrophilic *meso*-tetra(hydroxyphenyl)-2,3-dihydroxychlorin (THPC) to CLIO, which allowed for 3-fold greater nanoparticle loading.[73] The resulting CLIO-THPC had improved aqueous stability and almost 60 times greater phototoxicity than conventional chlorin e_6 (Figure 8). In an apolipoprotein E-deficient mouse model of atherosclerosis, CLIO-THPC localized to carotid artery atheroma (specifically areas rich in macrophages and foam cells). Surgically exposed carotid arteries were irradiated with 650 nm light, incisions were closed, and mice were allowed to recuperate. Follow-up tissue staining showed extensive macrophage cell death and apoptosis in atheroma (Figure 8). CLIO-THPC caused significantly less skin phototoxicity in mice compared to chlorin e_6, validating the benefit of nanoparticle-targeted PDT.

7. Conclusions

The platform of dextran-coated iron oxide nanoparticles has proven to be an important part of the armamentarium for multiple phases of personalized medicine (i.e., therapy chosen to match individual genotype or phenotype). The large cargo capacity and suitability for a variety of conjugation methods has enabled CLIO's use for molecular imaging, sensitive and rapid ex vivo detection of analytes, and the targeted delivery of therapy. Ongoing and future efforts will extend the lessons learned with CLIO to clinical grade iron oxide nanoparticles, such as those based on ferumoxides, ferumoxtran-10, or ferumoxytol. Also, the reproducible synthesis of derivatized nanoparticles designed for human applications needs to be standardized. Targeting ligands will be developed against a wider range of cellular proteins, enabling applications in a wider range of diseases. Finally, studies of nanoparticles in cohorts of human subjects are needed to rigorously assess the potential of these nanoparticles to function as clinically relevant biomarkers. Ultimately, these types of nanoparticles show great potential to participate in many steps in the cycle of personalized care, including individualized risk stratification, early diagnosis,

and assessment of disease activity. Such personalized phenotyping can subclassify patients to identify new endophenotypes, and match patients with the most appropriate therapy.

BIOGRAPHICAL INFORMATION

Carlos Tassa is a Research Scientist in the Center for Systems Biology at Massachusetts General Hospital (MGH). He received his B.S and M.S. in Chemistry from the University of Massachusetts Boston, working under the guidance of John C. Warner. Following his Ph.D. studies in synthetic organic chemistry at Dartmouth College with Peter A. Jacobi, he pursued post doctoral training in the Chemical Biology Program at the Broad Institute of Harvard and MIT under Stanley Shaw and Stuart Schreiber.

Stanley Y Shaw is a Principal Investigator and Co-Director of Chemical Biology in the MGH Center for Systems Biology and an Assistant Professor at Harvard Medical School. He received his A.B. in Chemistry & Physics, M.D. and Ph.D. at Harvard; his Ph.D. in Biophysics studied DNA topology under the supervision of James Wang. He worked with Stuart Schreiber as a Howard Hughes Medical Institute physician postdoctoral fellow. His laboratory seeks to develop a variety of approaches to phenotype human patients and correlate these phenotypes with their genetic susceptibility to disease. These goals are pursued using molecular imaging, phenotyping of patient-derived cells, chemical biology, and extracting phenotypes from electronic health records (EHR) using natural language processing.

Ralph Weissleder is a Professor of Systems Biology and of Radiology at Harvard Medical School and Director of the Center for Systems Biology at Massachusetts General Hospital (MGH). Dr. Weissleder is a graduate of the University of Heidelberg. He has received many awards including the J. Taylor International Prize in Medicine, the Millenium Pharmaceuticals Innovator Award, the AUR Memorial Award, the ARRS President's Award, The Society for Molecular Imaging Lifetime Achievement Award, and the Academy of Molecular Imaging 2006 Distinguished Basic Scientist Award. In 2009 he was elected to the Institute of Medicine in the United States National Academies. His lab has been a driving force in studying human biology using molecular imaging and nanotechnology, with a particular focus on cancer and inflammatory diseases. He has developed systematic ways to explore disease biology using in vivo imaging and has been instrumental in translating several discoveries into new drugs.

The authors gratefully acknowledge the contributions from all researchers whose work has been described in this Account. This work was funded by Contract Number HHSN268201000044C (NIH/NHLBI) to S.Y.S. and R.W.

FOOTNOTES

*To whom correspondence should be addressed. E-mail: rweissleder@mgh.harvard.edu.

REFERENCES

1 Jaffer, F. A.; Weissleder, R. Molecular imaging in the clinical arena. *JAMA, J. Am. Med. Assoc.* **2005**, *293* (7), 855–862.

2 McCarthy, J. R.; Weissleder, R. Multifunctional magnetic nanoparticles for targeted imaging and therapy. *Adv. Drug Delivery Rev.* **2008**, *60* (11), 1241–1251.

3 Weissleder, R. Molecular imaging in cancer. *Science* **2006**, *312* (5777), 1168–1171.

4 Shen, T.; Weissleder, R.; Papisov, M.; Bogdanov, A. J.; Brady, T. J. Monocrystalline iron oxide nanocompounds (MION): physicochemical properties. *Magn. Reson. Med.* **1993**, *29* (5), 599–604.

5 Weissleder, R.; Bogdanov, A.; Neuwelt, E. A.; Papisov, M. Long-circulating iron oxides for MR imaging. *Adv. Drug Delivery Rev.* **1995**, *16*, 321–334.

6 Harisinghani, M. G.; Barentsz, J.; Hahn, P. F.; Deserno, W. M.; Tabatabaei, S.; van de Kaa, C. H.; de la Rosette, J.; Weissleder, R. Noninvasive detection of clinically occult lymph-node metastases in prostate cancer. *N. Engl. J. Med.* **2003**, *348* (25), 2491–2499.

7 Weissleder, R.; Stark, D. D.; Engelstad, B. L.; Bacon, B. R.; Compton, C. C.; White, D. L.; Jacobs, P.; Lewis, J. Superparamagnetic iron oxide: pharmacokinetics and toxicity. *AJR, Am. J. Roentgenol.* **1989**, *152* (1), 167–173.

8 Josephson, L.; Tung, C. H.; Moore, A.; Weissleder, R. High-efficiency intracellular magnetic labeling with novel superparamagnetic-Tat peptide conjugates. *Bioconjugate Chem.* **1999**, *10* (2), 186–191.

9 Wunderbaldinger, P.; Josephson, L.; Weissleder, R. Crosslinked iron oxides (CLIO): a new platform for the development of targeted MR contrast agents. *Acad Radiol.* **2002**, *9* (Suppl 2), S304–6.

10 Park, J.; An, K.; Hwang, Y.; Park, J. G.; Noh, H. J.; Kim, J. Y.; Park, J. H.; Hwang, N. M.; Hyeon, T. Ultra-large-scale syntheses of monodisperse nanocrystals. *Nat. Mater.* **2004**, *3* (12), 891–895.

11 Sun, S.; Zeng, H.; Robinson, D. B.; Raoux, S.; Rice, P. M.; Wang, S. X.; Li, G. Monodisperse MFe_2O_4 (M = Fe, Co, Mn) nanoparticles. *J. Am. Chem. Soc.* **2004**, *126* (1), 273–279.

12 Hyeon, T.; Lee, S. S.; Park, J.; Chung, Y.; Na, H. B. Synthesis of highly crystalline and monodisperse maghemite nanocrystallites without a size-selection process. *J. Am. Chem. Soc.* **2001**, *123* (51), 12798–12801.

13 Park, J.; Joo, J.; Kwon, S. G.; Jang, Y.; Hyeon, T. Synthesis of monodisperse spherical nanocrystals. *Angew. Chem., Int. Ed.* **2007**, *46* (25), 4630–4660.

14 Lee, H.; Yoon, T. J.; Figueiredo, J. L.; Swirski, F. K.; Weissleder, R. Rapid detection and profiling of cancer cells in fine-needle aspirates. *Proc. Natl. Acad. Sci. U.S.A.* **2009**, *106* (30), 12459–12464.

15 Weissleder, R.; Moore, A.; Mahmood, U.; Bhorade, R.; Benveniste, H.; Chiocca, E. A.; Basilion, J. P. In vivo magnetic resonance imaging of transgene expression. *Nat. Med.* **2000**, *6* (3), 351–355.

16 Devaraj, N. K.; Keliher, E. J.; Thurber, G. M.; Nahrendorf, M.; Weissleder, R. 18F labeled nanoparticles for in vivo PET-CT imaging. *Bioconjugate Chem.* **2009**, *20* (2), 397–401.

17 Harisinghani, M.; Ross, R. W.; Guimaraes, A. R.; Weissleder, R. Utility of a new bolus-injectable nanoparticle for clinical cancer staging. *Neoplasia* **2007**, *9* (12), 1160–1165.

18 Liong, M.; Shao, H.; Haun, J. B.; Lee, H.; Weissleder, R. Carboxymethylated polyvinyl alcohol stabilizes doped ferrofluids for biological applications. *Adv. Mater.* **2010**, *22* (45), 5168–5172.

19 Blackman, M. L.; Royzen, M.; Fox, J. M. Tetrazine ligation: fast bioconjugation based on inverse-electron-demand Diels-Alder reactivity. *J. Am. Chem. Soc.* **2008**, *130* (41), 13518–13519.

20 Devaraj, N. K.; Upadhyay, R.; Haun, J. B.; Hilderbrand, S. A.; Weissleder, R. Fast and sensitive pretargeted labeling of cancer cells through a tetrazine/trans-cyclooctene cycloaddition. *Angew. Chem., Int. Ed.* **2009**, *48* (38), 7013–7016.

21 Devaraj, N. K.; Weissleder, R.; Hilderbrand, S. A. Tetrazine-based cycloadditions: application to pretargeted live cell imaging. *Bioconjugate Chem.* **2008**, *19* (12), 2297–2299.

22 Haun, J. B.; Devaraj, N. K.; Hilderbrand, S. A.; Lee, H.; Weissleder, R. Bioorthogonal chemistry amplifies nanoparticle binding and enhances the sensitivity of cell detection. *Nat. Nanotechnol.* **2010**, *5* (9), 660–665.

23 Haun, J. B.; Devaraj, N. K.; Marinelli, B. S.; Lee, H.; Weissleder, R. Probing intracellular biomarkers and mediators of cell activation using nanosensors and bioorthogonal chemistry. *ACS Nano* **2011**, *5* (4), 3204–3213.

24 Han, H. S.; Devaraj, N. K.; Lee, J.; Hilderbrand, S. A.; Weissleder, R.; Bawendi, M. G. Development of a bioorthogonal and highly efficient conjugation method for quantum dots using tetrazine-norbornene cycloaddition. *J. Am. Chem. Soc.* **2010**, *132* (23), 7838–7839.

25 Keliher, E. J.; Reiner, T.; Turetsky, A.; Hilderbrand, S. A.; Weissleder, R. High-Yielding, Two-Step (18) F Labeling Strategy for (18) F-PARP1 Inhibitors. *ChemMedChem* **2011**, *6* (3), 424–427.

26 Reiner, T.; Earley, S.; Turetsky, A.; Weissleder, R. Bioorthogonal small-molecule ligands for PARP1 imaging in living cells. *ChemBioChem.* **2010**, *11* (17), 2374–2377.

27 Reiner, T.; Keliher, E. J.; Earley, S.; Marinelli, B.; Weissleder, R. Synthesis and In Vivo Imaging of a (18) F-Labeled PARP1 Inhibitor Using a Chemically Orthogonal Scavenger-Assisted High-Performance Method. *Angew. Chem., Int. Ed.* **2011**, *50* (8), 1922–1925.

28 Devaraj, N. K.; Hilderbrand, S.; Upadhyay, R.; Mazitschek, R.; Weissleder, R. Bioorthogonal Turn-On Probes for Imaging Small Molecules inside Living Cells. *Angew. Chem., Int. Ed.* **2010**, *49* (16), 2869–2872.

29 Weissleder, R.; Kelly, K.; Sun, E. Y.; Shtatland, T.; Josephson, L. Cell-specific targeting of nanoparticles by multivalent attachment of small molecules. *Nat. Biotechnol.* **2005**, *23* (11), 1418–1423.

30 Leimgruber, A.; Berger, C.; Cortez-Retamozo, V.; Etzrodt, M.; Newton, A. P.; Waterman, P.; Figueiredo, J. L.; Kohler, R. H.; Elpek, N.; Mempel, T. R.; Swirski, F. K.; Nahrendorf, M.; Weissleder, R.; Pittet, M. J. Behavior of endogenous tumor-associated macrophages assessed in vivo using a functionalized nanoparticle. *Neoplasia* **2009**, *11* (5), 459–468; 2 p following 468.

31 Kelly, K. A.; Shaw, S. Y.; Nahrendorf, M.; Kristoff, K.; Aikawa, E.; Schreiber, S. L.; Clemons, P. A.; Weissleder, R. Unbiased discovery of in vivo imaging probes through in vitro profiling of nanoparticle libraries. *Integr. Biol.* **2009**, *1* (4), 311–317.

32 Mammem, M.; Choi, S. K.; Whitesides, G. M. Polyvalent interactions in biological systems: implications for design and use of multivalent ligands and inhibitors. *Angew. Chem., Int. Ed.* **1998**, *21*, 2754–2794.

33 Tassa, C.; Duffner, J. L.; Lewis, T. A.; Weissleder, R.; Schreiber, S. L.; Koehler, A. N.; Shaw, S. Y. Binding affinity and kinetic analysis of targeted small molecule-modified nanoparticles. *Bioconjugate Chem.* **2010**, *21* (1), 14–19.

34 Thurber, G. M.; Schmidt, M. M.; Wittrup, K. D. Factors determining antibody distribution in tumors. *Trends Pharmacol. Sci.* **2008**, *29* (2), 57–61.

35 Sosnovik, D. E.; Nahrendorf, M.; Weissleder, R. Magnetic nanoparticles for MR imaging: agents, techniques and cardiovascular applications. *Basic Res. Cardiol.* **2008**, *103* (2), 122–130.

36 Tsourkas, A.; Josephson, L. Magnetic nanoparticles. In *Molecular Imaging: Principles and Practice*; Weissleder, R., Ross, B. D., Rehemtulla, A., Gambhir, S. S., Eds.; People's Medical Publishing House: Shelton, CT, USA, 2010; pp 523−541.

37 Perez, J. M.; Josephson, L.; O'Loughlin, T.; Hogemann, D.; Weissleder, R. Magnetic relaxation switches capable of sensing molecular interactions. *Nat. Biotechnol.* **2002**, *20* (8), 816–820.

38 Lee, H.; Sun, E.; Ham, D.; Weissleder, R. Chip-NMR biosensor for detection and molecular analysis of cells. *Nat. Med.* **2008**, *14* (8), 869–874.

39 Lee, H.; Yoon, T. J.; Weissleder, R. Ultrasensitive detection of bacteria using core-shell nanoparticles and an NMR-filter system. *Angew. Chem., Int. Ed.* **2009**, *48* (31), 5657–5660.

40 Perez, J. M.; Josephson, L.; Weissleder, R. Use of magnetic nanoparticles as nanosensors to probe for molecular interactions. *ChemBioChem* **2004**, *5* (3), 261–264.

41 Grimm, J.; Perez, J. M.; Josephson, L.; Weissleder, R. Novel nanosensors for rapid analysis of telomerase activity. *Cancer Res.* **2004**, *64* (2), 639–643.

42 Kaittanis, C.; Naser, S. A.; Perez, J. M. One-step, nanoparticle-mediated bacterial detection with magnetic relaxation. *Nano Lett.* **2007**, *7* (2), 380–383.

43 Perez, J. M.; Grimm, J.; Josephson, L.; Weissleder, R. Integrated nanosensors to determine levels and functional activity of human telomerase. *Neoplasia* **2008**, *10* (10), 1066–1072.

44 Kaittanis, C.; Nath, S.; Perez, J. M. Rapid nanoparticle-mediated monitoring of bacterial metabolic activity and assessment of antimicrobial susceptibility in blood with magnetic relaxation. *PLoS One* **2008**, *3* (9), e3253.

45 Haun, J. B.; Yoon, T. J.; Lee, H.; Weissleder, R. Magnetic nanoparticle biosensors. *Wiley Interdiscip. Rev.: Nanomed. Nanobiotechnol.* **2010**, *2* (3), 291–304.

46 Kaittanis, C.; Santra, S.; Perez, J. M. Role of nanoparticle valency in the nondestructive magnetic-relaxation-mediated detection and magnetic isolation of cells in complex media. *J. Am. Chem. Soc.* **2009**, *131* (35), 12780–12791.

47 Kaittanis, C.; Banerjee, T.; Santra, S.; Santiesteban, O. J.; Teter, K.; Perez, J. M. Identification of molecular-mimicry-based ligands for cholera diagnostics using magnetic relaxation. *Bioconjugate Chem.* **2011**, *22* (2), 307–314.

48 Haun, J. B.; Castro, C. M.; Wang, R.; Peterson, V. M.; Marinelli, B. S.; Lee, H.; Weissleder, R. Micro-NMR for Rapid Molecular Analysis of Human Tumor Samples. *Sci. Transl. Med.* **2011**, *3* (71), 71ra16.

49 Denis, M. C.; Mahmood, U.; Benoist, C.; Mathis, D.; Weissleder, R. Imaging inflammation of the pancreatic islets in type 1 diabetes. *Proc. Natl. Acad. Sci. U.S.A.* **2004**, *101* (34), 12634–12639.

50 Guimaraes, A. R.; Rakhlin, E.; Weissleder, R.; Thayer, S. P. Magnetic resonance imaging monitors physiological changes with antihedgehog therapy in pancreatic adenocarcinoma xenograft model. *Pancreas* **2008**, *37* (4), 440–444.

51 Guimaraes, A. R.; Ross, R.; Figuereido, J. L.; Waterman, P.; Weissleder, R. MRI with Magnetic Nanoparticles Monitors Downstream Anti-Angiogenic Effects of mTOR Inhibition. *Mol. Imaging Biol.* **2010**, *13* (2), 314–320.

52 Hogemann, D.; Ntziachristos, V.; Josephson, L.; Weissleder, R. High throughput magnetic resonance imaging for evaluating targeted nanoparticle probes. *Bioconjugate Chem.* **2002**, *13* (1), 116–121.

53 Sosnovik, D. E; Weissleder, R. Emerging concepts in molecular MRI. *Curr. Opin. Biotechnol.* **2007**, *18* (1), 4–10.

54 Jaffer, F. A.; Nahrendorf, M.; Sosnovik, D.; Kelly, K. A.; Aikawa, E.; Weissleder, R. Cellular imaging of inflammation in atherosclerosis using magnetofluorescent nanomaterials. *Mol. Imaging* **2006**, *5* (2), 85–92.

55 Kelly, K. A.; Bardeesy, N.; Anbazhagan, R.; Gurumurthy, S.; Berger, J.; Alencar, H.; Depinho, R. A.; Mahmood, U.; Weissleder, R. Targeted nanoparticles for imaging incipient pancreatic ductal adenocarcinoma. *PLoS Med.* **2008**, *5* (4), e85.

56 Korosoglou, G.; Tang, L.; Kedziorek, D.; Cosby, K.; Gilson, W. D.; Vonken, E. J.; Schar, M.; Sosnovik, D.; Kraitchman, D. L.; Weiss, R. G.; Weissleder, R.; Stuber, M. Positive contrast MR-lymphography using inversion recovery with ON-resonant water suppression (IRON). *J. Magn. Reson. Imaging.* **2008**, *27* (5), 1175–1180.

57 Korosoglou, G.; Weiss, R. G.; Kedziorek, D. A.; Walczak, P.; Gilson, W. D.; Schar, M.; Sosnovik, D. E.; Kraitchman, D. L.; Boston, R. C.; Bulte, J. W.; Weissleder, R.; Stuber, M. Noninvasive detection of macrophage-rich atherosclerotic plaque in hyperlipidemic rabbits using "positive contrast" magnetic resonance imaging. *J. Am. Coll. Cardiol.* **2008**, *52* (6), 483–491.

58 Montet, X.; Weissleder, R.; Josephson, L. Imaging pancreatic cancer with a peptide-nanoparticle conjugate targeted to normal pancreas. *Bioconjugate Chem.* **2006**, *17* (4), 905–911.

59 Morishige, K.; Kacher, D. F.; Libby, P.; Josephson, L.; Ganz, P.; Weissleder, R.; Aikawa, M. High-resolution magnetic resonance imaging enhanced with superparamagnetic nanoparticles measures macrophage burden in atherosclerosis. *Circulation* **2010**, *122* (17), 1707–1715.

60 Nahrendorf, M.; Jaffer, F. A.; Kelly, K. A.; Sosnovik, D. E.; Aikawa, E.; Libby, P.; Weissleder, R. Noninvasive vascular cell adhesion molecule-1 imaging identifies inflammatory activation of cells in atherosclerosis. *Circulation* **2006**, *114* (14), 1504–1511.

61 Schellenberger, E. A.; Sosnovik, D.; Weissleder, R.; Josephson, L. Magneto/optical annexin V, a multimodal protein. *Bioconjugate Chem.* **2004**, *15* (5), 1062–1067.

62 Sosnovik, D. E.; Garanger, E.; Aikawa, E.; Nahrendorf, M.; Figuiredo, J. L.; Dai, G.; Reynolds, F.; Rosenzweig, A.; Weissleder, R.; Josephson, L. Molecular MRI of cardiomyocyte apoptosis with simultaneous delayed-enhancement MRI distinguishes apoptotic and necrotic myocytes in vivo: potential for midmyocardial salvage in acute ischemia. *Circ. Cardiovasc. Imaging* **2009**, *2* (6), 460–467.

63 Sosnovik, D. E.; Nahrendorf, M.; Panizzi, P.; Matsui, T.; Aikawa, E.; Dai, G.; Li, L.; Reynolds, F.; Dorn, G. W. n.; Weissleder, R.; Josephson, L.; Rosenzweig, A. Molecular MRI detects low levels of cardiomyocyte apoptosis in a transgenic model of chronic heart failure. *Circ. Cardiovasc. Imaging* **2009**, *2* (6), 468–475.

64 Sosnovik, D. E.; Schellenberger, E. A.; Nahrendorf, M.; Novikov, M. S.; Matsui, T.; Dai, G.; Reynolds, F.; Grazette, L.; Rosenzweig, A.; Weissleder, R.; Josephson, L. Magnetic resonance imaging of cardiomyocyte apoptosis with a novel magneto-optical nanoparticle. *Magn. Reson. Med.* **2005**, *54* (3), 718–724.

65 Turvey, S. E.; Swart, E.; Denis, M. C.; Mahmood, U.; Benoist, C.; Weissleder, R.; Mathis, D. Noninvasive imaging of pancreatic inflammation and its reversal in type 1 diabetes. *J. Clin. Invest.* **2005**, *115* (9), 2454–2461.

66 Nahrendorf, M.; Keliher, E.; Marinelli, B.; Waterman, P.; Feruglio, P. F.; Fexon, L.; Pivovarov, M.; Swirski, F. K.; Pittet, M. J.; Vinegoni, C.; Weissleder, R. Hybrid PET-optical imaging using targeted probes. *Proc. Natl. Acad. Sci. U.S.A.* **2010**, *107* (17), 7910–7915.

67 Nahrendorf, M.; Keliher, E.; Marinelli, B.; Leuschner, F.; Robins, C. S.; Gerszten, R. E.; Pittet, M. J.; Swirski, F. K.; Weissleder, R. Detection of Macrophages in Aortic Aneurysms by Nanoparticle Positron Emission Tomography-Computed Tomography. *Arterioscler., Thromb., Vasc. Biol.* **2011**, *31* (4), 750–757.

68 Santra, S.; Kaittanis, C.; Grimm, J.; Perez, J. M. Drug/dye-loaded, multifunctional iron oxide nanoparticles for combined targeted cancer therapy and dual optical/magnetic resonance imaging. *Small* **2009**, *5* (16), 1862–1868.

69 Kievit, F. M; Zhang, M. Surface Engineering of Iron Oxide Nanoparticles for Targeted Cancer Therapy. *Acc. Chem. Res.* **2011**, DOI: 10.1021/ar2000277.

70 Ethirajan, M.; Chen, Y.; Joshi, P.; Pandey, R. K. The role of porphyrin chemistry in tumor imaging and photodynamic therapy. *Chem. Soc. Rev.* **2011**, *40* (1), 340–362.

71 Spikes, J. D. Chlorins as photosensitizers in biology and medicine. *J. Photochem. Photobiol., B* **1990**, *6* (3), 259–274.

72 McCarthy, J. R.; Jaffer, F. A.; Weissleder, R. A macrophage-targeted theranostic nanoparticle for biomedical applications. *Small* **2006**, *2* (8−9), 983–987.

73 McCarthy, J. R.; Korngold, E.; Weissleder, R.; Jaffer, F. A. A light-activated theranostic nanoagent for targeted macrophage ablation in inflammatory atherosclerosis. *Small* **2010**, *6* (18), 2041–2049.